

## Exact period-three solutions in the delayed logistic map

María Belén D'Amico<sup>†</sup>, Guillermo L. Calandrini<sup>†‡</sup> and Jorge L. Moiola<sup>†</sup>

<sup>†</sup>Instituto de Investigaciones en Ingeniería Eléctrica - IIIE (UNS-CONICET)

Dto. de Ing. Eléctrica y de Computadoras, Universidad Nacional del Sur  
 Avda Alem 1253, B8000CPB Bahía Blanca, Argentina

<sup>‡</sup>Departamento de Matemática, Universidad Nacional del Sur  
 Avda Alem 1253, B8000CPB Bahía Blanca, Argentina

Email: mbdamico@uns.edu.ar, calandri@criba.edu.ar, jmoiola@uns.edu.ar

**Abstract**—Analytical and exact solutions of the period-three orbits exhibited by the delayed logistic map are presented. Expressions are obtained by applying the harmonic balance method and Gröbner bases to an equivalent single-input single-output representation of the system. A detailed study of the effect of the delays on the appearance of bistability phenomenon is also included.

### 1. Introduction

There exists a great variety of discrete maps coming from different branches of science which develop a period doubling (PD) cascade as one of the parameters is varied. Among the extensive list of examples, it can be mentioned: population models in Biology [1, 2], cardiac activity models in Medicine [3], structure markets in Economics [4], impact systems in Mechanics [5], the modulated lasers in Physics [6, 7], etc. In many of these applications, logistic map has played a remarkable role in the description of the dynamical scenarios.

Classical cascades consist in the successive unfolding of PD bifurcations leading to the existence of period- $2^k$  ( $k > 1$ ) orbits around the fixed point. This sequence conforms a widely-known route to chaos [8, 9]. Once the chaotic scenario is achieved, dynamics alternates between *periodic* and *chaotic windows*. Perhaps, the most singular periodic window is the one originated by a period-three (P3) saddle-node bifurcation. In scalar maps, it gives rise to the noted phrase “*period-three implies chaos*” [10].

In the chaos control technique proposed by Pyragas [11], unstable periodic orbits inside the cascade can be stabilized by using time-delayed versions of the states in the feedback loop. Besides its simplicity, this controller can provoke the appearance of the so-called bistability phenomenon [12]. Thus, for example, it is possible to find that P3 orbits coexist with the desired dynamics. Due to the inherent increase in the dimension of the systems, these nonlinear phenomena are usually study by making numerical simulations [7].

In this paper, P3 orbits exhibited by the delayed version of the logistic map are characterized analytically. Developments are based on an input-output representation of the system, a Fourier decomposition of the orbit and a balance of the involved harmonics [13]. Exact solutions of the

periodic points are obtained for any arbitrary delay value. This is possible thanks to the application of Gröbner bases to the resulting set of polynomials [14]. Results complement those presented in [15] concerning the appearance of period-four oscillations in a family of quadratic maps. Previous analytical developments related to periodic orbits in the scalar logistic map can be found in [16, 17].

The paper is organized as follows. In Section 2, the equivalent input-output representation of the delayed logistic map is described. The set of polynomials with triangular structure that permits to obtain the exact expressions of the P3 orbits is presented in Section 3. Critical conditions for the appearance of these solutions as a function of the time delays are included in Section 4. Finally, conclusions are summarized in Section 5.

### 2. Input-output representation

The delayed version of the logistic map is given by

$$x_{k+1} = \alpha x_k(1 - x_k) - \eta(x_{k-\sigma} - x_k), \quad (1)$$

where  $\alpha$  is the growth rate of the original system ( $\alpha \geq 1$ ),  $\eta$  is the control gain ( $-1 < \eta < 1$ ) and  $\sigma$  is the proposed delay in time ( $\sigma \geq 1$ ). The control term implies an increase in the dimension of the system. In fact, (1) can be rewritten as the  $(\sigma + 1)$ -dimensional state-variable map

$$x_{k+1} = Ax_k + B[\alpha y_k^2 - (\alpha + \eta)y_k], \quad (2)$$

where  $y_k = Cx_k$  and

$$A = \begin{pmatrix} 0 & -\eta \\ I_{\sigma \times \sigma} & 0 \end{pmatrix}, \quad B^T = C = \begin{pmatrix} 1 & 0 & \cdots & 0 \end{pmatrix}.$$

This extension can be overcome representing the map as the Lure system of Fig. 1 consisting of a dynamical linear block  $G(\cdot)$  connected to a nonlinear and static function  $f(\cdot)$  by means of a feedback loop. The variables are input  $v_k$ , error  $e_k$  and output  $y_k$ . Since  $v_k$  is assumed to be zero, the input of  $G(\cdot)$  is directly  $u_k = -f(y_k)$ .

Following routine calculations and applying the  $z$ -transform, the equivalent input-output representation is

$$G(z) = \frac{z^\sigma}{z^{\sigma+1} + \eta}, \quad (3)$$

$$f(y_k) = \alpha y_k^2 - (\alpha + \eta)y_k. \quad (4)$$

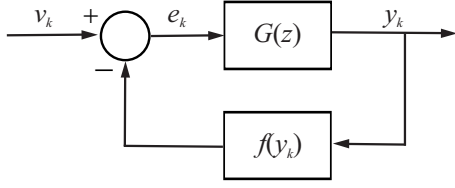


Figure 1: Input-output representation.

Notice that  $G(z)$  is a scalar rational function,  $y_k \in \mathbf{R}$  and  $f(\cdot) : \mathbf{R} \rightarrow \mathbf{R}$ . Thus, the  $(\sigma + 1)$ -dimensional original system reduces to an interconnection between two scalar functions independently of the arbitrary delay value.

Fixed points are obtained via the equation  $\widehat{y} = -G(1)f(\widehat{y})$  where  $G(1) = 1/(1 + \eta)$  is the response of linear block to frequency  $\omega = 0$  ( $z = e^{i0} = 1$ ). As it is known, the Pyragas control law maintains the fixed points of the original map, i.e.  $\widehat{y}_- = 1 - 1/\alpha$  and  $\widehat{y}_+ = 0$ . The stability of each  $\widehat{y}_\pm$  is determined by means of the open-loop function  $G(z)J$  where  $J = D_y f(\widehat{y}_\pm) = 2\alpha\widehat{y}_\pm - (\alpha + \eta)$ . In particular, if  $G(e^{i\omega})J = -1 + i0$  for certain  $\omega = \omega_o$ , the fixed point will change its stability condition [13]. Thus, it can be affirmed that  $\widehat{y}_+$  is always unstable but the dynamical scenario around  $\widehat{y}_-$  depends on the gain and delay values.

As it is shown in [15], delayed logistic map develops PD bifurcations but the characteristics of respective P2 orbits depends on the  $\sigma$  parity. In fact, the critical condition is equal to that of the original map ( $\alpha = 3$ ) for even  $\sigma$  values while it is changed to  $\alpha = 3 + 2\eta$  for odd  $\sigma$  values, modifying the interval where  $\widehat{y}_-$  is stable. Period-three solutions exhibited by (1) are analyzed in the following. The equivalent input-output representation will facilitate the application of the harmonic balance method for the characterization of these orbits.

### 3. Exact period-three solutions

The Fourier decomposition of a P3 orbit can be expressed as

$$y_k = \widehat{y} + Y_0 + Y_3 e^{i\frac{2\pi}{3}k} + \overline{Y}_3 e^{-i\frac{2\pi}{3}k}, \quad (5)$$

where  $\widehat{y} = \widehat{y}_-$ ,  $Y_0 \in \mathbf{R}$  is a correction of  $\widehat{y}$  to achieve the center or average value  $\overline{Y}_0 = \widehat{y} + Y_0$  of the oscillation and  $Y_3 = Y_{3R} + iY_{3I} \in \mathbf{C}$ , together with its conjugate  $\overline{Y}_3$ , represents the amplitude of the unique harmonic  $e^{i2\pi/3k}$ . Thus, the three periodic points are:  $y_1 = \widehat{y} + Y_0 - Y_{3R} - \sqrt{3}Y_{3I}$ ,  $y_2 = \widehat{y} + Y_0 - Y_{3R} + \sqrt{3}Y_{3I}$  and  $y_3 = \widehat{y} + Y_0 + 2Y_{3R}$ .

Considering that (5) is the input of the nonlinear block (4), the respective output  $f(y_k)$  is calculated. Making some algebraic manipulations, it is obtained

$$f(y_k) = f(\widehat{y}) + F_0 + F_3 e^{i\frac{2\pi}{3}k} + \overline{F}_3 e^{-i\frac{2\pi}{3}k},$$

where

$$F_0 = (\alpha - 2 - \eta)Y_0 + \alpha(Y_0^2 + 2|Y_3|^2), \quad (6)$$

$$F_3 = (\alpha - 2 - \eta)Y_3 + \alpha(2Y_0Y_3 + \overline{Y}_3^2). \quad (7)$$

As can be seen,  $f(y_k)$  preserves the harmonic decomposition of the proposed  $y_k$ . Since  $e_k = -f(y_k)$  is the input of the linear block  $G(\cdot)$ , the loop in Fig. 1 is closed by establishing the harmonic balance

$$Y_0 = -G(1)F_0, \quad (8)$$

$$Y_3 = -G(e^{i\frac{2\pi}{3}})F_3, \quad (9)$$

where  $G(e^{i\frac{2\pi}{3}})$  is the response of  $G(\cdot)$  at a frequency  $\omega = 2\pi/3$  ( $z = e^{i2\pi/3}$ ).

Combining (6) to (9), it results a set of two polynomials in the complex variables  $Y_0$  and  $Y_3$ . Assuming that  $G(e^{i\frac{2\pi}{3}})J \neq -1 + i0$  (since resonances 1:3 are not analyzed) and denoting  $G_1 = G(1)$  and  $G(e^{i\frac{2\pi}{3}}) = G_{\frac{\pi}{3}R} + iG_{\frac{\pi}{3}I}$ , balance equations can be transformed into three polynomials in  $Y_0$ ,  $Y_{3R}$  and  $Y_{3I}$  with real coefficients given by

$$\begin{aligned} Y_0 &= -G_1(\alpha - 2 - \eta)Y_0 + G_1\alpha(Y_0^2 + 2Y_{3R}^2 + 2Y_{3I}^2), \\ Y_{3R} &= -G_{\frac{\pi}{3}R}[(\alpha - 2 - \eta)Y_{3R} + \alpha(2Y_0Y_{3R} + Y_{3R}^2 - Y_{3I}^2)] \\ &\quad + G_{\frac{\pi}{3}I}[(\alpha - 2 - \eta)Y_{3I} + \alpha(2Y_0Y_{3I} - 2Y_{3R}Y_{3I})], \\ Y_{3I} &= -G_{\frac{\pi}{3}R}[(\alpha - 2 - \eta)Y_{3I} + \alpha(2Y_0Y_{3I} - 2Y_{3R}Y_{3I})] \\ &\quad - G_{\frac{\pi}{3}I}[(\alpha - 2 - \eta)Y_{3R} + \alpha(2Y_0Y_{3R} + Y_{3R}^2 - Y_{3I}^2)]. \end{aligned}$$

Due to the involved complexity, the real roots of the resulting polynomial system are found by using Gröbner bases. This algebraic algorithm generates a new polynomial set with the same ideal to that of the original one, preserving the same roots [14]. To facilitate the algebraic manipulation,  $Y_0$  is replaced by  $\overline{Y}_0 - \widehat{y}$ . Thus, it is defined the set of polynomials  $P = \{p_1, p_2, p_3\}$  with

$$\begin{aligned} p_1 &= [1 - (\alpha + \eta)G_1]\overline{Y}_0 + \alpha G_1\overline{Y}_0^2 + 2\alpha G_1Y_{3R}^2 + 2\alpha G_1Y_{3I}^2, \\ p_2 &= [1 - (\alpha + \eta)G_{\frac{2\pi}{3}R}]Y_{3R} + (\alpha + \eta)G_{\frac{2\pi}{3}I}Y_{3I} + 2\alpha G_{\frac{2\pi}{3}R}\overline{Y}_0Y_{3R} \\ &\quad - 2\alpha G_{\frac{2\pi}{3}I}\overline{Y}_0Y_{3I} + 2\alpha G_{\frac{2\pi}{3}I}Y_{3R}Y_{3I} + \alpha G_{\frac{2\pi}{3}R}Y_{3R}^2 - \alpha G_{\frac{2\pi}{3}R}Y_{3I}^2, \\ p_3 &= [1 - (\alpha + \eta)G_{\frac{2\pi}{3}R}]Y_{3I} - (\alpha + \eta)G_{\frac{2\pi}{3}I}Y_{3R} + 2\alpha G_{\frac{2\pi}{3}R}\overline{Y}_0Y_{3I} \\ &\quad - 2\alpha G_{\frac{2\pi}{3}R}Y_{3R}Y_{3I} + 2\alpha G_{\frac{2\pi}{3}I}\overline{Y}_0Y_{3R} + \alpha G_{\frac{2\pi}{3}I}Y_{3R}^2 - \alpha G_{\frac{2\pi}{3}I}Y_{3I}^2. \end{aligned}$$

Fixing the variable order  $\overline{Y}_0 < Y_{3R} < Y_{3I}$  and considering the coefficients in  $P$  are rational functions of the parameters, a Gröbner basis composed by four polynomials is obtained. The one depending on  $\overline{Y}_0$  can be factorized as  $0 = \overline{Y}_0(1 - \alpha + \alpha\overline{Y}_0)g_0$  where

$$\begin{aligned} g_0 &= 2G_1[1 - 2(\alpha + \eta)G_{\frac{2\pi}{3}R} + (\alpha + \eta)^2|G(e^{i\frac{2\pi}{3}})|^2] \\ &\quad + \alpha[8G_1G_{\frac{2\pi}{3}R} + (1 - 9(\alpha + \eta)G_1)|G(e^{i\frac{2\pi}{3}})|^2]\overline{Y}_0 \\ &\quad + 9\alpha^2G_1|G(e^{i\frac{2\pi}{3}})|^2\overline{Y}_0^2. \end{aligned}$$

Only the roots of  $g_0$  correspond to the P3 orbits since they are solutions of  $P = \mathbf{0}$  for  $Y_{3R} \neq 0$  and  $Y_{3I} \neq 0$ . The rest are solutions of  $P = \mathbf{0}$  for  $Y_{3R} = Y_{3I} = 0$ . So, to find the expressions of the Fourier coefficients representing the P3

Table 1: Frequency response for different delay values

Delays (mod 3)	$G_{\frac{2\pi}{3}R}$	$G_{\frac{2\pi}{3}I}$
$\sigma \equiv 0$	$\frac{-\frac{1}{2}+\eta}{1-\eta+\eta^2}$	$\frac{-\frac{\sqrt{3}}{2}}{1-\eta+\eta^2}$
$\sigma \equiv 1$	$-\frac{1+\eta}{2(1-\eta+\eta^2)}$	$\frac{-\sqrt{3}(1-\eta)}{2(1-\eta+\eta^2)}$
$\sigma \equiv 2$	$-\frac{1+\eta}{2(1+2\eta+\eta^2)}$	$-\frac{\sqrt{3}(1+\eta)}{2(1+2\eta+\eta^2)}$

solutions, the algebraic algorithm is applied again but now to  $\widetilde{P} = P \cup g_0$ . Thus, the Gröbner basis reduces to three polynomials with triangular structure  $\{g_0, g_{3R}, g_{3I}\}$  where

$$\begin{aligned}
 g_{3R} = & G_1(\alpha + \eta)[11(\alpha + \eta)G_1 - 32]G_{\frac{2\pi}{3}R}|G(e^{i\frac{2\pi}{3}})|^2 \\
 & + G_1(\alpha + \eta)^2[16 - 9(\alpha + \eta)G_1]|G(e^{i\frac{2\pi}{3}})|^4 \\
 & - G_1^2(7G_{\frac{2\pi}{3}R} - 5(\alpha + \eta)G_{\frac{2\pi}{3}R}^2 + 9(\alpha + \eta)G_{\frac{2\pi}{3}I}^2) \\
 & + 16G_1|G(e^{i\frac{2\pi}{3}})|^2 - 2\alpha \left[ G_1^2(5G_{\frac{2\pi}{3}R}^2 - 9G_{\frac{2\pi}{3}I}^2) - 4|G(e^{i\frac{2\pi}{3}})|^4 \right. \\
 & \left. - 9G_1(\alpha + \eta)[(\alpha + \eta)G_1 - 2]|G(e^{i\frac{2\pi}{3}})|^4 \right. \\
 & \left. - 10G_1G_{\frac{2\pi}{3}R}|G(e^{i\frac{2\pi}{3}})|^2 \right] \widetilde{Y}_0 - 27\alpha G_1^2|G(e^{i\frac{2\pi}{3}})|^2 Y_{3R} \\
 & + 27\alpha(\alpha + \eta)G_1^2|G(e^{i\frac{2\pi}{3}})|^2 \left[ 2G_{\frac{2\pi}{3}R} - (\alpha + \eta)|G(e^{i\frac{2\pi}{3}})|^2 \right] Y_{3R} \\
 & - 108\alpha^2 G_1^2 G_{\frac{2\pi}{3}R}|G(e^{i\frac{2\pi}{3}})|^2 \widetilde{Y}_0 Y_{3R} \\
 & + 108\alpha^2 G_1|G(e^{i\frac{2\pi}{3}})|^4 \widetilde{Y}_0 Y_{3R} - 324\alpha^3 G_1^2|G(e^{i\frac{2\pi}{3}})|^4 Y_{3R}^3, \\
 g_{3I} = & G_1 \left[ 1 - 2(\alpha + \eta)G_{\frac{2\pi}{3}R} + (\alpha + \eta)^2|G(e^{i\frac{2\pi}{3}})|^2 \right] \\
 & + 4\alpha \left[ G_1 G_{\frac{2\pi}{3}R} - |G(e^{i\frac{2\pi}{3}})|^2 \right] \widetilde{Y}_0 - 9\alpha G_1 G_{\frac{2\pi}{3}R} Y_{3R} \\
 & + 9\alpha G_1(\alpha + \eta)|G(e^{i\frac{2\pi}{3}})|^2 Y_{3R} - 18\alpha^2 G_1|G(e^{i\frac{2\pi}{3}})|^2 \widetilde{Y}_0 Y_{3R} \\
 & - 18\alpha^2 G_1|G(e^{i\frac{2\pi}{3}})|^2 Y_{3R}^2 - 9\alpha G_1 G_{\frac{2\pi}{3}I} Y_{3I},
 \end{aligned}$$

and main coefficients are not zero since  $G_1 \neq 0$  and resonance 1:3 ( $G_{\frac{2\pi}{3}I} \neq 0$ ) is omitted.

Polynomial  $g_0$  corresponds to the  $\widetilde{Y}_0$  solutions. The others two permit the calculation of  $Y_{3R}$  and  $Y_{3I}$  recursively. Notice that there could exist up to two possible solutions of  $\widetilde{Y}_0$  and, for each of them, up to three values of  $Y_{3R}$  and  $Y_{3I}$ . The exact amount of real solutions is determined by the sign of the discriminant of the polynomials.

#### 4. Delay dependence

The linear dynamical function (3) evaluated at  $\omega = 2\pi/3$  is given by  $G_{\frac{2\pi}{3}} = e^{i\sigma\frac{2\pi}{3}} / (e^{i(\sigma+1)\frac{2\pi}{3}} + \eta)$ . Since  $\omega = 2\pi/3$  corresponds to the complex third root of unity and also  $e^{i\sigma\frac{2\pi}{3}} = e^{i(\widetilde{\sigma}+3s)\frac{2\pi}{3}} = e^{i\widetilde{\sigma}\frac{2\pi}{3}}$  with  $\widetilde{\sigma} = 0, 1, 2$  and  $s \in \mathbf{Z}$ ,  $G_{\frac{2\pi}{3}}$  presents three types of responses according to the  $\sigma$  values in modulus 3, as listed in Table 1. This implies that the discriminant of  $g_0$ , denoted as  $\Delta_{\widetilde{Y}_0}$ , reduces to the three different expressions given in Table 2. In all cases, it can be affirmed that the delayed map does not present P3 orbits whenever  $\Delta_{\widetilde{Y}_0} < 0$ , since there do not exist real  $\widetilde{Y}_0$  solutions.

Table 2: Critical conditions for the onset of P3 orbits

Delays (mod 3)	$\Delta_{\widetilde{Y}_0} = 0$
$\sigma \equiv 0$	$\alpha - 1 - 2\sqrt{2} = 0$
$\sigma \equiv 1$	$\alpha - 1 - 2\sqrt{2}\sqrt{1 - \eta + \eta^2} = 0$
$\sigma \equiv 2$	$\alpha - 1 - 2\sqrt{2}\sqrt{1 + 2\eta + \eta^2} = 0$

For  $\Delta_{\widetilde{Y}_0} \geq 0$ , the two  $\widetilde{Y}_0$  solutions are real. Now, for those parameter combinations, it also occurs that the discriminant of  $g_{3R}$  is different from zero. In fact,  $g_{3R}$  always has three real roots. So, the two roots of  $\widetilde{Y}_0$  plus the three roots of  $Y_{3R}$  ( $Y_{3I}$ ) conform the six periodic points involved in the two different P3 orbits (one stable and one unstable) of the system. Therefore, expression  $\Delta_{\widetilde{Y}_0} = 0$  can be seen as the critical condition for the occurrence of the defined P3 saddle-node bifurcation.

Critical curves in the plane  $(\alpha, \eta)$  indicating the appearance of the PD bifurcation (starting point of the PD cascade) and the P3 saddle-node bifurcation for different delays are depicted in Figs. 2(a)-(b). The dynamical scenario is equal to that of the original logistic map only for even  $\sigma$  values congruent with 0 [Fig. 2(a)]. For even delays congruent with 1, the P3 saddle-node bifurcation emerges after the PD cascade, but, at lower (higher)  $\alpha$  values when  $\eta > 0$  ( $\eta < 0$ ). For even delays congruent with 2, there exist two possible scenarios: P3 orbits occur after the PD cascade ( $\eta > 0$ ) or they coexist with stable attractors such as P2 orbits or the fixed point ( $\eta < 0$ ).

Bistability phenomena can also be detected for odd  $\sigma$  values [Fig. 2(b)]. In this case, P3 orbits coexist with different stable attractors when delays are congruent with 0 or 1 and  $\eta > 0$ . Figure 3 illustrates the coexistence of stable P2 and P3 orbits for  $\sigma = 1$  and  $\eta = 0.2$ . For odd delays congruent with 2, the P3 saddle-node bifurcation goes always after the PD cascade, occurring at lower (higher)  $\alpha$  values respect to  $1 + 2\sqrt{2}$  when  $\eta < 0$  ( $\eta > 0$ ).

#### 5. Conclusions

Exact expressions of the P3 orbits exhibited by the delayed logistic map have been obtained. Results are based on a simple input-output representation of the system, the Fourier decomposition of the orbit and the application of the harmonic balance method. The reduced set of quadratic polynomials is solved by using Gröbner bases.

Analytical results permit to formalize conditions for the appearance of bistabilities. Period-three attractors can coexist with the stable fixed point and even with other stable periodic orbits for even delays congruent with 2 (mod 3). In the case of odd delays, bistable scenarios occur whenever  $\sigma$  values are congruent with 0 or 1 (mod 3).

**Acknowledgments:** Authors acknowledge the financial support of UNS (PGI 24/K064), CONICET (PIP 112-201201-00062) and ANCyT (PICT-2014-2161).

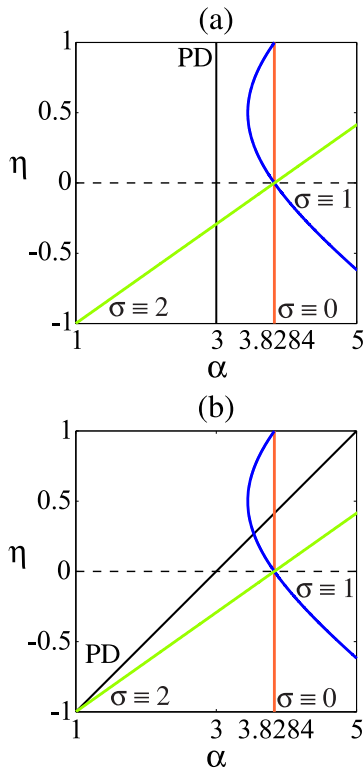


Figure 2: Critical curves corresponding to PD and P3 saddle-node bifurcations: (a) even delays; (b) odd delays.

### References

- [1] Peng M. “Multiple bifurcations and periodic bubbling in a delay population model”, *Chaos, Solitons Fractals*, vol. 25, pp. 1123–1130, 2005.
- [2] Jing Z. and Yang J., “Bifurcation and chaos in discrete-time predator-prey system”, *Chaos, Solitons Fractals*, vol. 27, pp. 259–277, 2006.
- [3] Brandt M. E. and Chen G., “Feedback control of a quadratic map model of cardiac chaos”, *Int. J. Bif. and Chaos*, vol. 6, No. 4, pp. 715–723, 1996.
- [4] Agiza H. N. and Elsadany A. A., “Chaotic dynamics in nonlinear duopoly game with heterogeneous players”, *Appl. Math. Comp.*, vol. 149, pp. 843–860, 2004.
- [5] Luo G. W. and Xie J. H., “Stability of periodic motion, bifurcations and chaos of a two-degree-of-freedom vibratory system with symmetrical rigid stops”, *J. Sound Vibration*, vol. 273, pp. 543–568, 2004.
- [6] Pieroux D. and Erneux T., “Minimal model of a class-B laser with delayed feedback: Cascading branching of periodic solutions and period-doubling bifurcation”, *Phys. Rev. A*, vol. 50, No. 2, pp. 1822–1829, 1994.
- [7] Martínez-Zérega B. E., Pisarchik A. N. and Tsimring L. S., “Using periodic modulation to control coex-

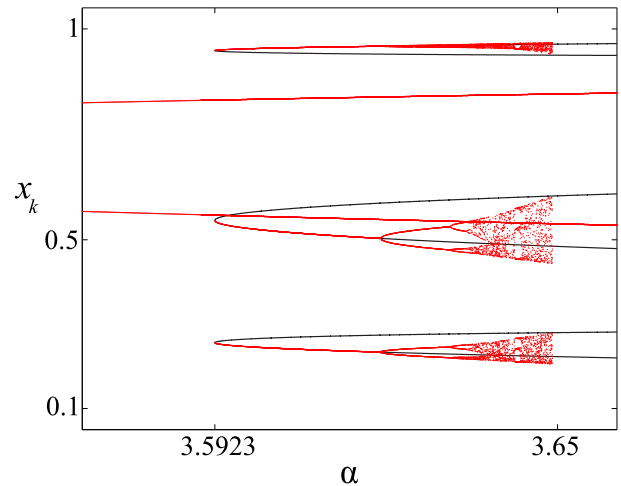


Figure 3: Coexistence of P3 and P2 orbits for  $\sigma = 1$  and  $\eta = 0.2$ . Red: numerical simulations; black: exact solutions.

isting attractors induced by delayed feedback”, *Phys. Lett. A*, vol. 318, pp. 102–111, 2003.

- [8] Strogatz S., *Nonlinear Dynamics and Chaos*, Westview Press, Colorado, 2001.
- [9] Sander E. and Yorke J., “Connecting period-doubling cascades to chaos”, *Int. J. Bifurcation Chaos*, vol. 22, No. 2, art. 1250022, 2012.
- [10] Li T.-Y. and Yorke J. A., “Period three implies chaos”, *The American Math. Monthly*, vol. 82, No. 10, pp. 985–992, 1975.
- [11] Pyragas K., “Continuous control of chaos by self-controlling feedback”, *Phys. Lett. A*, vol. 170, pp. 421–428, 1992.
- [12] Pisarchik A. N. and Feudel U., “Control of multistability”, *Phys. Reports*, vol. 540, pp. 167–218, 2014.
- [13] Gentile F. S., Bel A. L., D’Amico M. B. and Muiola J. L., “Effect of delayed feedback on the dynamics of a scalar map via a frequency-domain approach”, *Chaos*, vol. 21, No. 2, art. 023117, 2011.
- [14] Cox D., J. Little y D. O’Shea (2007). *Ideals, Varieties, and Algorithms*, 3rd edition, Springer, New York.
- [15] D’Amico M. B. and Calandrini G. L., “Exact period-four solutions of a family of n-dimensional quadratic maps via harmonic balance and Gröbner bases”, *Chaos*, under review, 2015.
- [16] Saha P. and Strogatz S. H., “The birth of period three”, *Math. Magazine*, vol. 68, no. 1, pp. 42–47, 1995.
- [17] Kotsireas I. S. and Karamanos K., “Exact computation of the bifurcation point  $B_4$  of the logistic map and the Bailey-Broadhurst conjectures”, *Int. J. Bifurcation Chaos*, vol. 14, No. 7, pp. 2417–2423, 2004.